DESIGN OF THE TARGET DUMP INJECTION SEGMENTED (TDIS) IN THE FRAMEWORK OF THE HIGH LUMINOSITY LARGE HADRON COLLIDER (HL-LHC) PROJECT

L. Teofili[*,1,2], M. Migliorati[1,2], Sapienza University of Rome, Rome, Italy
D. Carbajo, I. Lamas, A. Perillo, CERN, Geneva, Switzerland
[1]also at CERN, Geneva, Switzerland; [2]also at INFN, Rome, Italy

Abstract

The High Luminosity Large Hadron Collider (HL-LHC) Project at CERN calls for increasing beam brightness and intensity. In this scenario, most equipment has to be re-designed and rebuilt. In particular, beam intercepting devices (such as dumps, collimators, absorbers and scrapers) have to withstand impact or scraping of the new intense HL-LHC beams without failure. Furthermore, minimizing the electromagnetic beam-device interactions is also a key design driver since they can lead to beam instabilities and excessive thermo-mechanical loading of devices. In this context, the present study assesses the conceptual design quality of the new LHC injection protection absorber, the Target Dump Injection Segmented (TDIS), from an electromagnetic and thermo-mechanical perspective. This contribution analyzes the thermo-mechanical response of the device considering two cases: an accidental beam impact scenario and another accidental scenario with complete failure of the RF-contacts. In addition, this paper presents the preliminary results from the simulation of the energy deposited by the two counter-rotating beams circulating in the device.

INTRODUCTION

The CERN accelerator complex has been undergoing upgrades to improve its performance. In the framework of the LIU (LHC Injection Upgrade) [1] and HL-LHC (High Luminosity LHC) [2] projects, an increase of the beam brightness and intensity is foreseen [1]. Several systems have to be redesigned and rebuilt to survive the new demanding situation. This is particularly true for the beam intercepting devices (BIDs), such as dumps, collimators, absorbers and scrapers [3], since they have to deal with two main beam intensity related phenomena:

- Nuclei-Matter Interactions (NMI). BIDs are usually responsible for absorbing a large part of the beam energy (beam dumping) or for the beam scraping, i.e. the removal of the unstable peripheral beam particles (beam halos). Thus, they are directly exposed to beam impacts and particle irradiation. It is well known that the incidence of the proton beam on the device material results in an energy deposition in the material itself and that this effect increases linearly with the beam intensity.

- Electromagnetic Beam-Device Interactions. BIDs usually operate in close proximity to the particle beam. In

this context, if the device impedance (the electromagnetic beam-device coupling index) is not minimized, they will experience strong electromagnetic interaction with the beam circulating in the accelerator. This interaction causes an energy deposition in the equipment (RF-Heating), proportional to the square of the beam intensity and to the device impedance [4].

The induced energy deposition on the BIDs may lead to an uneven temperature distribution, the resulting thermal gradients can generate high mechanical stresses, potentially causing material failure or other undesired effects [5–7].

The higher HL-LHC beams intensity will increase the energy deposited in equipment by NMI and RF-Heating. Thus, these phenomena needs to be carefully accounted for during the design of the new BIDs. Their thermo-mechanical effects must be investigated through a series of simulations. Thus, the present work reports the results of the studies performed to assess the electro-thermo-mechanical behaviour of the new LHC injection protection absorber, the Target Dump Injection Segmented (TDIS) [8], see Fig. 1.

The first section of this contribution describes the scope of the device, its functionality, its location in the CERN accelerator complex and its geometry. Subsequently, the results of the electromagnetic and thermo-mechanical simulations are shown. Two worst case scenarios are discussed. Case one: beam impacting on the device. Case two: complete failure of the RF-contacts, i.e. maximum RF-heating load. Finally, the paper presents the preliminary strategy for simulating the power dissipated by the two counter-rotating beams circulating in the device.

THE TDIS

The TDIS is a dump/absorber aimed at protecting downstream LHC equipment during the injection phase. Since the LHC stores two counter rotating beams, two of these devices will be installed in the machine. They will be located in the LHC ring, immediately downstream of the connection between the transfer line from Super Proton Synchrotron (SPS)-to-LHC [8], in order to absorb the injected beam in case of an injection kicker malfunctions [9]. Furthermore, the device will be used as a dump for the proton beam during commissioning operations [9].

The TDIS has been developed as an improved version of the current absorber, Target Dump Injection (TDI) [8]. In 2015 and in the LHC first operational run (2009-2013), the TDI experienced severe issues, as structural damage and
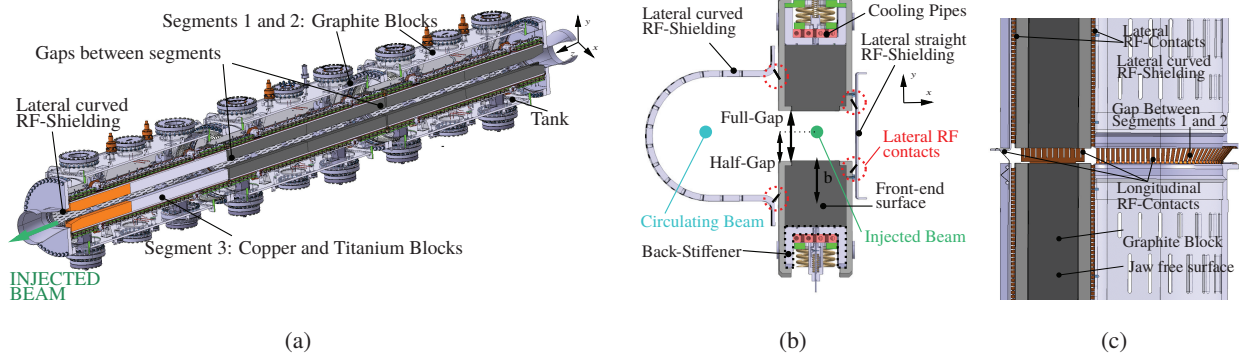
Figure 1: (a) Complete TDIS design Geometry. (b) Section view in *x-y* plane. The main components are labeled. (c) Section view in *x-z* plane. The main components are labeled.

jaws deformations [10]. These issues are believed to be due to unexpected, excessive RF-Heating [6]. To avoid such problems, in the TDIS a new system of RF-contacts and RF-shielding (see Fig. 1b and 1c) will be implemented. It will allow an impedance reduction with respect to the TDI, a crucial requirement to decrease the RF-heating load of the high intensity/brightness HL-LHC beams [11].

The geometry of the TDIS is presented in Fig. 1 and described in detail in [8]. The core of the TDIS are two vertically movable jaws (upper and lower jaw), divided into three segments, each of them composed of absorbing blocks of different materials. The three segments of a jaw are separated by gaps of 15 mm (see Fig. 1a and 1c). This arrangement limits jaw bending and deformation allowing unconstrained thermal expansion at the gaps. This makes the TDIS design mechanically more robust if compared with the TDI.

In the TDIS there are two counter rotating beams circulating at all time: the injected beam that is passing between the jaws and the circulating one traversing the device in the RF-screen, Fig. 1b. During the injection phase the jaws have a half-gap of 4 mm with respect to the injected beam reference orbit (golden orbit), refer to Fig. 1b. If the orbit of the actual injected beam differs more than the allowed tolerance, it will impact against the jaws so it is dumped. After the injection phase the jaws are completely open (half gap 55 mm) [9].

THE ACCIDENTAL BEAM IMPACT SCENARIO

The TDIS will cope with different failure scenarios of the SPS-to-LHC injection magnet [9] that can arise during the injection phase until the LHC ring is completely filled. In such failure cases, the proton beam is misdirected resulting in an impact against the absorbing blocks of the TDIS jaws [12]. Two main types of accidents could occur during the lifespan of the device. They are defined by the impact parameter *b*, the distance between the beam impact position and the jaw free surface, (Fig. 1b).

- Grazing (small impact parameter, $0\sigma_y \le b \le 1\sigma_y$, where σ_y is the transverse root mean square beam dimension on the *y* axis): the proton beam impacts the graphite block at a small depth (compared to the beam core dimension) with respect to the jaw free surface. Most of the energy is deposited on the material surface.

- Central impact (large impact parameter, $b >> \sigma_y$): the proton beam impacts the front end of the graphite block. Most of the energy is deposited in the material bulk.

Furthermore, in both cases only one jaw, either the upper or lower one is expected to receive the beam impact. Thus, the thermo-mechanical response of only one jaw has been investigated. The jaw model is shown in Fig. 1b. The beam-matter interaction was simulated using the FLUKA Monte Carlo code [13, 14]. Subsequently, the 3D dissipated energy density map, obtained from FLUKA, was imported as a thermal load into the software ANSYS® [15], to analyze the thermo-mechanical behavior of the device.

Both in the grazing impact scenario and in the central impact one the first jaw segment experienced the highest temperatures and stresses. The thermal analysis revealed that a grazing impact may lead to a rise of the absorbing blocks temperature up to 1392°C in the first impacted graphite block (see Fig. 2) whilst the other jaw components experience a negligible increase in temperature. This is due to the fact that most of the energy is deposited in the graphite block, on its jaw free surface, far from other components. A temperature of 1392°C is not critical for the graphite, as it can tolerate up to 2800°C [16]. Mechanical studies have shown that the maximum mechanical stresses induced by the thermal gradients are also localized in the first graphite block. Since graphite is a brittle material, the Christensen criterion [17] was used to assess its mechanical resistance. The local Christensen coefficient is shown for the graphite block in Fig. 3. The fact that this coefficient remains locally below 1 guarantees the mechanical robustness of the block, provided that the principal stresses are lower than the compressive and tensile limits of the material.

Regarding the central impact scenario, the thermal analysis has shown that the most dangerous thermal gradient
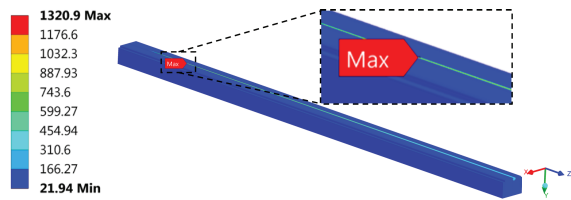
TUP2WE04

Figure 2: Surface temperature [°C] of the graphite block due to grazing impact. The high temperature is extremely localized on a longitudinal line in the jaw free surface.
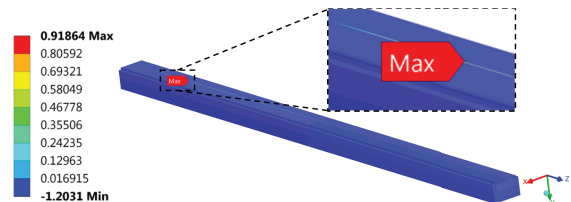

Figure 3: Christensen coefficient [adimensional unit] on the graphite block due to grazing impact. A value superior or equal to 1 implies material failure. However, 0.91 is acceptable because of the conservative assumption of considering the static yield stress at room temperature as maximum tensile limits. Indeed, the static yield stress for the graphite increases with temperature in this temperature range [18]. Like the high temperature, the stresses are also extremely localized on a longitudinal line in the free jaw surface.
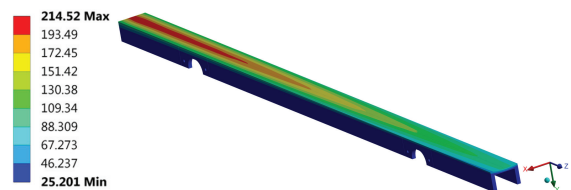

Figure 4: Surface temperature [°C] of the back stiffener due to the particle shower after the central impact.
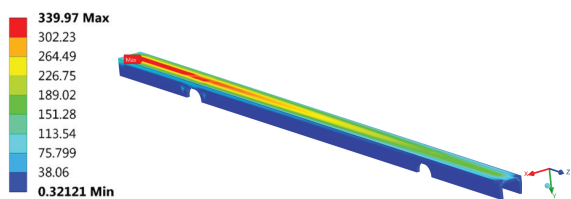

Figure 5: Surface Stresses [MPa] of the back stiffener due to the thermal gradient.

develops in the molybdenum alloy (TZM) back-stiffener, which reaches a peak temperature of 215°C (see Fig. 1b and 4), and in the oxygen-free copper cooling pipes (see Fig. 1b), which reaches a peak temperature of 92°C. Mechanical analyses have revealed significant stresses in these two key components. They have shown that the pipes are likely to undergo some minor plastic deformation as a consequence of the thermal gradients caused by the particle shower energy deposition. However, this is not expected to be detrimental for the device function, given the high ductility of the

material. For the back-stiffener, the Finite Element Analysis (FEA) shows that, in the event of a central impact, it will be subjected to mechanical stresses of 340 MPa. This stress value is below the elastic limit of the material for that temperature which is 455 MPa [18] (resulting in a safety margin of 1.33). It must be noted that this is a conservative approach. Indeed, the energy deposition due to the beam impact is very localized in space and takes place in an extremely short time scale (strain rate 1.610^2 [s^{-1}]). Thus, a dynamic behavior for the TZM must be considered, i.e. elastic waves are generated in the material because of the sudden sharp temperature increase and the induced localized material expansion immediately after the beam impact [5]. In this case, the maximum stress obtained by the simulation must be compared with the dynamic yield strength for TZM, which is significantly larger than the static one [19].

COMPLETE RF-CONTACT FAILURE SCENARIO

To minimize the TDIS impedance, and so the RF-heating, four main elements are present in the device design: the lateral curved RF-shielding, the lateral straight RF-shielding, the longitudinal RF-contacts and the lateral RF-contacts (see Fig.1). The RF-contacts keep the electrical connection of all the device components, allowing the image currents (a flow of electrons induced by the beam electromagnetic field in the device walls) to flow easily. The shielding modifies the geometry seen by the beam in order to avoid the excitation of electromagnetic high order resonant modes (HOM) in the device structure. The overall effect of these components is a low impedance for the TDIS as shown in detail in the work of Teofili et al. [20]. In the same work the thermo-mechanical effects of the RF-heating and of the secondary beam halos are also discussed in the case of complete failure of the longitudinal RF-finger in the device. Thus, since in this paper the whole TDIS project is discussed, for the sake of completeness, the main results are summarized. In case of complete failure of the longitudinal RF-contacts, for a jaws half-gap of 4 mm, electromagnetic simulations performed by CST studio suite® [21] have shown that High Order Modes (HOMs) can develop in the structure at frequencies of 0.75 GHz and higher. Since the HL-LHC beams spectrum has a frequency content up to 1.5 GHz, the HOMs between 0.75 and 1.50 GHz are excited. Considering only the injected beam as a source of HOMs excitation, the power dissipated is 1003 W, (the two beam case scenario is considered in the next section). Moreover, the RF-heating due to resistive wall impedance has to be considered, a further 798 W. Finally, 580 W, due to the interaction between the secondary beam halos and the jaws, needs to be added. These thermal loads occur simultaneously and continuously during the injection phase, which can last up to 45 minutes. The thermo-mechanical simulations have shown a high temperature, 293°C, around the longitudinal gaps between the TDIS modules whereas the maximum stresses are on the lateral RF-shielding, at the connection with the tank. However, the
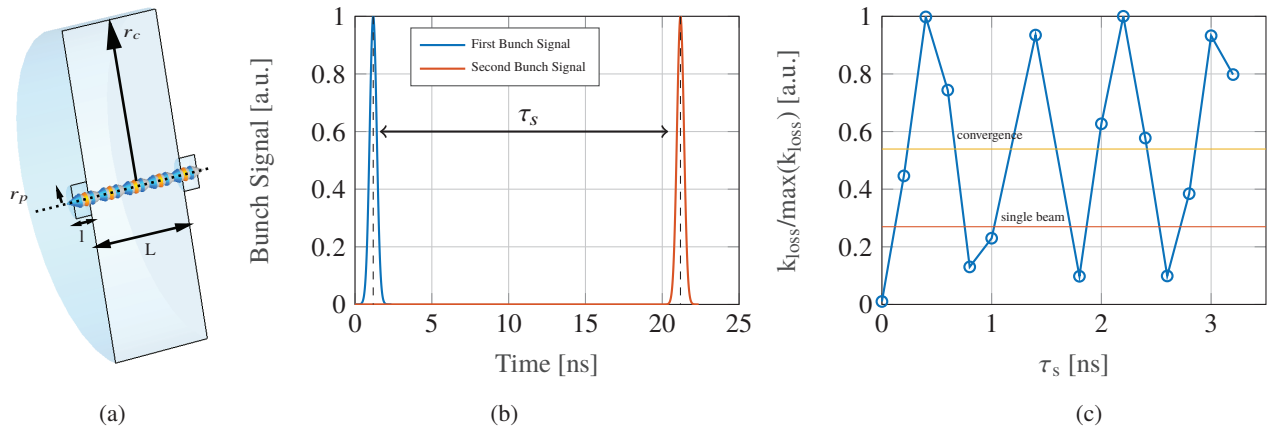
Figure 6: (a) Simulated cavity model with geometrical entities: r_c = 100 mm, r_p = 10 mm, L = 60 mm, l = 10 mm. (b) Gaussian bunch signal, the time delay τ_s is indicated. (c) Normalized energy loss factor [adimensional unit] for different time delays τ_s between bunches computed for an electrical conductivity of the wall of 10^{-3} S/m. The convergence value is reported (the constant value of the energy loss factor of the two beam for $\tau_s > 100$ ns). Furthermore, also the energy loss of a single beam ($q = 4.5 \ 10^{-8}$ C, σ = 70 mm) passing in the structure is plotted.

maximum von Mises stress value (85 MPa) is well below the static yield strength of the material (250 MPa for stainless steel) and the temperatures reached are not dangerous for the material.

FUTURE STRATEGY FOR RF-HEATING LOAD DUE TO DOUBLE BEAM

Another scenario to be investigated carefully is the one in which the TDIS operates in nominal conditions. In this case there is no failure in any of the device components, the injected beam is passing in its golden orbit between the jaws (the latter has a half-gap of 4 mm) and the circulating beam traverses the TDIS at the center of the curved RF-shielding. In this framework, it is crucial to consider as simultaneous source of heating the two beams. The main heat load mechanisms are still NMI and RF-heating. The contribution of NMI is expected to be unchanged with respect to the already discussed case of complete RF-contacts failure (580 W for 45 minutes) whereas, this is not the case for the RF-Heating. Indeed, the NMI contribution mainly arises from the interaction of the injected beam secondary halos with the close jaws; the circulating beam is too far from the TDIS components to deposit a significant amount of energy due to NMI. Regarding the RF-heating, both beams act as a source of excitation for HOMs in the structure; thus, they both contribute to the energy deposition. Unfortunately, while the problem of the energy deposition due to the device impedance for a single beam has been rigorously investigated [4], the same problem for a double beam has remained relatively unexplored and is still unsolved for the general case. The pioneering study of C. Zannini, G. Rumolo and G. Iadarola [22] has solved it for a simple pipe geometry. It seems to indicate an interference-like behaviour of the RF deposited energy in the considered structure dependent on the time delay between the entrance of the first and the second beam in the device, τ_s (see Fig. 6b). Thus, the RF-heating load of two counter-rotating beams in a worst case scenario could be up to four times the heat load induced in the same device by a single beam. In order to benchmark this thesis for more complex geometries the pill-box cavity represented in Fig. 6a was simulated with the software CST particle studio. Using the Wakefield solver [23] the passage of two counter rotating beams, both positioned exactly at the center of the structure was modelled. Both beams were composed of only one gaussian bunch with a charge $q = 4.5 \ 10^{-8}$ C and a root mean square σ_t = 70 mm. The first beam entered the structure at time $t_1 = 0$ s, while the second one entered with an arbitrary delay τ_s (see Fig. 6b). Computing the total energy loss factor for every τ_s as a sum of the loss factors of the two beams, the results shown in Fig. 6c were obtained,. In the same figure the normalized energy loss factor of a single beam traversing the structure is also represented. It is possible to notice the oscillating, interference-like, behaviour, i.e. the deposited energy of two counter rotating beams passing in the pill-box have peaks four times higher than the energy deposited in the same pill-box by a single beam. Furthermore, simulations not reported in this work displayed that for high values of τ_s, more than 100 ns with a wall conductivity $\sigma = 10^{-3}$ S/m, there is no more oscillations in the loss factor. It converges to a value that is the double of the loss factor of a single beam. This is because, with the considered value of the electrical conductivity σ, the resonant electric field induced by the first bunch is completely decayed after 100 ns. Thus, the second bunch experiences the same initial condition than the first one and generates the same energy loss. Thus, as can be easily seen, the simulation results, for the particular case proposed, validate the thesis of an interference like behaviour of the deposited energy for two counter-rotating beams. Please note that the results shown in this section are preliminary and neglect various aspects, for instance the fact that in the

real case the two counter rotating beams cannot share the exact same orbit. However, they are encouraging as they reveal the capability of the CST software to simulate this kind of phenomenon. Additionally, they can be used to have an initial estimate of the total deposited energy in a device given a delay τ_s between the beams entrance in the structure. Further investigations are currently on going at CERN with the goal of better understanding the phenomenon and of obtaining a general solution of the two counter rotating beam energy deposition problem, valid also for complex geometries.

CONCLUSION

In this work we reviewed the electromagnetic and thermo-mechanical analysis performed to assess the quality of the new Target Dump Injection Segmented. In particular, we discussed two critical scenarios: an accidental case of beam impact on the device and another accidental case of complete longitudinal RF-contacts failure. In both cases, the design was found to be robust and capable of withstanding the generated temperatures and stresses. Furthermore, another possible critical scenario was outlined. It is the one in which the device operates in nominal conditions and the two beams that are passing through it are both considered as a source of RF-heating loads. This problem was found unsolved in the literature in the general case. Hence, this study analized it for the simple case of a pill-box, obtaining an interference like behaviour for the deposited energy. Future work will try to extend such a results for more complex cases, investigating a possible analytic solution.

ACKNOWLEDGMENTS

REFERENCES

[1] J. Coupard *et al.*, "LHC Injectors Upgrade Projects at CERN", in *Proc. 7th Int. Particle Accelerator Conf. (IPAC'16)*, Busan, Korea, May 2016, paper MOPOY059, pp. 992–995.

[2] G. Apollinari, A. Bejar, O. Bruning, M. Lamont, and L. Rossi, "High-Luminosity Large Hadron Collider (HL-LHC) : Preliminary Design Report", CERN, Geneva, Switzerland, Rep. CERN-2015-005, Dec. 2015.

[3] Beam Intercepting Design Review, https://en-sti-tcd.web.cern.ch/en-sti-tcd/html/equipment.html

[4] M. Furman, H. Lee, and B. Zotter, "Energy loss of bunched beams in RF cavities", Lawrence Berkeley National Laboratory, Berkeley, California, Rep. SSC-086, 1986.

[5] A. Bertarelli, "Beam Induced Damage Mechanisms and Their Calculation", in *Joint International Accelerator School: Beam Loss and Accelerator Protection*, Newport Beach, CA, USA, 5–14 Nov. 2014, edited by R. Schmidt, CERN-2016-002 (CERN, Geneva, 2016), pp. 159–227.

[6] B. Salvant *et al.*, "Beam Induced RF Heating in LHC in 2005", in *Proc. 7th Int. Particle Accelerator Conf. (IPAC'16)*, Busan, Korea, May 2016, paper MOPOR008, pp. 602–605.

[7] D. Lipka, "Heating of a DCCT and a FCT due to wake losses in PETRAIII, simulations and solutions", presented at the Simulation of Power Dissipation & Heating from Wake Losses Workshop, Diamond Light Source, Oxfordshire, UK, Jan. 2013, unpublished.

[8] D. Carbajo Perez *et al.*, "Operational Feedback and Analysis of Current and Future Designs of the Injection Protection Absorbers in the Large Hadron Collider at CERN", in *Proc. 8th Int. Particle Accelerator Conf. (IPAC'17)*, Copenhagen, Denmark, May 2017, paper WEPVA108, pp. 3517–3520.

[9] C. Bracco, A. Lechner, D. Carbajo, and A. Perillo, "TDIS - Functional Specification", CERN, 2017, EDMS 1865250, to be released.

[10] A. Lechner *et al.*, "TDI - Past Observations and Improvements for 2016", in *Proc. Evian Workshop on LHC Beam Operations*, Evian, France, Dec. 2015, pp. 123–129.

[11] C. Bracco, "The new injection protection dump TDI", CERN, 2016, EDMS 1936580, to be released.

[12] A. Lechner *et al.*, "Energy Deposition Studies for Fast Losses during LHC Injection Failures", CERN, Geneva, Switzerland, Rep. CERN-ACC-2013-0288, 2013.

[13] G. Battistoni *et al.*, "Overview of the FLUKA code", *Annals of Nuclear Energy*, vol. 82, pp. 10-18, 2015.

[14] A. Ferrari, P.R. Sala, A. Fassò, and J. Ranft, "FLUKA: a multi-particle transport code", Rep. CERN-2005-10, INFN/TC_05/11, SLAC-R-773.

[15] ANSYS, https://www.ansys.com/

[16] F.X. Nuiry *et al.*, "Low-Z material R&D application for Beam Intercepting Devices (BID) at CERN", presented at the 13th Int. Work. on Spallation Materials Technology, Chattanooga, USA, Nov. 2016.

[17] R.M. Chistensen, "A Two Property Yield, Failure (Fracture) Criterion for Homogeneous, Isotropic Materials", *J. Eng. Mater. Technol.*, 2004, vol. 126, pp. 45–52

[18] A. Bertarelli, A. Lafuente, F. Carra, and P. Gradassi, "TDI thermo-mechanical simualtions: Boron Nitride versus Graphite", presented at the 235th LHC machine commitee, Geneva, Switzerland, Sep. 2015.

[19] G. Filacchioni, E. Casagrande, U. De Angelis, G. De Santis, and D. Ferrara, "Effects of strain rate on tensile properties of TZM and Mo–5%Re", *Journal of Nuclear Materials*, vol. 307-311, Dec. 2002, pp. 705-709.

[20] L. Teofili *et al.*, "Analysis on the Mechanical effects induced by beam impedance heating on the HL-LHC Target Dump Injection Segmented (TDIS) absorber", presented at the 9th Int. Particle Accelerator Conf. (IPAC'18), Vancouver, Canada, May 2018, paper THPAK092.

[21] CST Studio Suite, https://www.cst.com/products/csts2

[22] C. Zannini, G. Rumolo, and G. Iadarola, "Power loss calculation in separated and common beam chambers of the LHC", CERN, Geneva, Switzerland, CERN-ACC-2014-0122, 2014.

[23] CST Studio Suite: Wakefield Solver, https://www.cst.com/products/cstps/solvers/wakefieldsolver